

# Photocatalytic mineralisation of humic acids using TiO<sub>2</sub> modified by tungsten dioxide/ hydrogen peroxide

Beata Tryba\*, Michał Piszcz, Ewa Borowiak-Paleń, Barbara Grzmil, Antoni W. Morawski

West Pomeranian University of Technology, Szczecin, Institute of Chemical Technology and Environment Engineering, ul. Pułaskiego 10, 70-322 Szczecin, Poland

\*Corresponding author: e-mail: beata.tryba@zut.edu.pl

TiO<sub>2</sub> of anatase structure was modified by tungsten dioxide and H<sub>2</sub>O<sub>2</sub> in order to obtain WO<sub>3</sub>-TiO<sub>2</sub> photocatalyst with enhanced photocatalytic activity under both, UV and artificial solar light irradiations. WO<sub>3</sub> was dissolved in 30% H<sub>2</sub>O<sub>2</sub> and mixed with TiO<sub>2</sub> in a vacuum evaporator at 70°C. Such modified TiO<sub>2</sub> was dried and then calcinated at 400 and 600°C.

The prepared samples and unmodified TiO<sub>2</sub> were used for the photocatalytic decomposition of humic acids (Leonardite standard IHSS) in the aqueous solution under irradiations of both, UV and artificial solar light. Modification of TiO<sub>2</sub> with tungsten dioxide and H<sub>2</sub>O<sub>2</sub> improved separation of free carriers in TiO<sub>2</sub> which resulted in the increase of OH radicals formation. Calcination caused an increase of anatase crystals and higher yield in OH radicals. The uncalcined samples showed high abilities for the adsorption of HA. Combination of adsorption abilities and photocatalytic activity of photocatalyst caused that the uncalcined TiO<sub>2</sub> modified with WO<sub>3</sub>/H<sub>2</sub>O<sub>2</sub> showed the shortest time of HA mineralisation. The mineralisation of HA under the artificial solar light was much lower than under the UV. It was proved that, although OH radicals are powerful in the decomposition of HA, adsorption can facilitate the contact of the adsorbed molecules with the photocatalyst surface and accelerate their photocatalytic decomposition.

**Keywords:** WO<sub>3</sub>/TiO<sub>2</sub>, humic acids photodecomposition, OH radicals formation.

## INTRODUCTION

Humic acids naturally present in the surface water state a problem because of their abilities to form the trihalomethanes (THMs) during the chlorination of water. THMs are classified as carcinogenic compounds<sup>1</sup>. The removal of humic acids by the conventional methods such as coagulation or filtration is not completely satisfactory, therefore the other solutions for HA destruction are searched and applied<sup>2</sup>. It has already been reported that humic acids (HA) could be efficiently removed from water through the photocatalytic process, which belongs to Advances Oxidation Processes<sup>3-8</sup>. Formed in these processes the hydroxyl radicals are strong oxidising species, which are responsible for the decomposition of organic matter in water. The OH radicals can be generated by ozonation, photolysis of H<sub>2</sub>O<sub>2</sub>, photo-Fenton reaction or photocatalysis, among these processes the last one is interesting because of the low cost of the photocatalyst used and the relative high efficiency. The most common photocatalyst tested for the photocatalytic decomposition of HA is TiO<sub>2</sub><sup>4-8</sup>. In a common photocatalytic process the UV irradiation is used for the excitation of TiO<sub>2</sub>, however solar light with a small content of UV rays (around 4%) is also applied. It was reported that artificial sunlight irradiation was not sufficient to cause a significant decomposition of HA, whereas TiO<sub>2</sub> appeared to be very effective under the UV irradiation<sup>8</sup>. The macromolecular humic acids on the visible light-illuminated TiO<sub>2</sub> are degraded with the reduction of aromatic character but not to the complete mineralization<sup>6</sup>. Many researchers noticed that HA are strongly adsorbed on the surface of TiO<sub>2</sub>, which has influence on the surface oxidative mechanism<sup>4-8</sup>. Some authors reported that the photodegradation of HA could proceed on the surface via the oxidation by hole and this mechanism was favoured in the case of the

adsorbed molecules<sup>5</sup>. HA was progressively degraded by the surface oxidative mechanism and so long as some macromolecules issued from HA remained in solution this mechanism predominated<sup>5</sup>. Some researchers prepared the composite of TiO<sub>2</sub> and granular activated carbon (GAC) in order to enhance the adsorption abilities of the photocatalyst. They reported that the degradation of HA on the TiO<sub>2</sub>/GAC composite was facilitated by the synergistic relationship between surface adsorption characteristics and photocatalytic potential<sup>7</sup>.

The disadvantage of using the TiO<sub>2</sub> photocatalyst is that only UV light can be applied for its excitation, because it has a relatively high value of the band gap energy, around 3.2 eV (for active anatase phase). The efficiency of TiO<sub>2</sub> photocatalyst can be increased by doping some metals as silver, gold or platinum, which are electron acceptors and can retard the inconvenient recombination reaction, which occurs in TiO<sub>2</sub> after its excitation, giving better separation of the free carriers and increasing the OH radicals formation<sup>9-11</sup>. Another solution of better photocatalytic performance is the preparation of a new generation of photocatalysts, which demonstrates activity under visible light. A lot of work was done to prepare non metal doping TiO<sub>2</sub> (incorporation of nitrogen, carbon, sulphur atoms, etc.)<sup>12-16</sup>.

The other possibility is the preparation of a mixture of two semiconductors with different energies of the band gap, such as TiO<sub>2</sub> doping with WO<sub>3</sub>. WO<sub>3</sub> has the value of the band gap energy about 2.8 eV and can absorb the light in the visible range. It was reported by Li and Song<sup>17-18</sup> that when the coupled photocatalyst WO<sub>3</sub>/TiO<sub>2</sub> was prepared by the sol-gel method, no stoichiometric solid solution of W<sub>x</sub>Ti<sub>1-x</sub>O<sub>2</sub> would be formed inside the forbidden band of TiO<sub>2</sub> which induces a tungsten impurity energy level responsible for the activity under visible light. Shifu et al.<sup>19</sup> reported

that when  $\text{WO}_3$  and  $\text{TiO}_2$  form a coupled photocatalyst,  $\text{TiO}_2$  and  $\text{WO}_3$  can be excited simultaneously under UV illumination. As the conduction band of  $\text{WO}_3$  is lower than that of  $\text{TiO}_2$ , the former can act as a sink for the photogenerated electrons. The photogenerated electrons of the  $\text{TiO}_2$  conduction band will be transferred to the conduction band of  $\text{WO}_3$ . Since the holes move in the opposite direction from the electrons, photogenerated holes might be trapped within the  $\text{TiO}_2$  particle, which makes charge separation more efficient<sup>19–25</sup>. A lot of methods of  $\text{WO}_3/\text{TiO}_2$  preparation have been used and reported on, such as impregnation, sol-gel, hydrothermal, sol-precipitation, ball milling, electro-deposition, metal ion implantation, etc.<sup>18–30</sup>.

In the presented manuscript photodecomposition of HA was performed on the prepared  $\text{WO}_3/\text{TiO}_2$  photocatalyst. For the preparation of  $\text{WO}_3/\text{TiO}_2$  the impregnation method was selected in order to obtain a good dispersion of tungsten oxide particles on the surface of  $\text{TiO}_2$ . Well dispersed  $\text{WO}_3$  particles on the surface of  $\text{TiO}_2$  can sufficiently retard the recombination reaction and increase the absorption of the visible light. We used this method, because we would like to use for the preparation a raw industrially produced  $\text{TiO}_2$  material, which has very high BET surface area, around  $300 \text{ m}^2/\text{g}$ . The disadvantage of this method consists in the fact that it does not allow the narrowing of the band gap by introducing the tungsten oxide phase inside the forbidden band of  $\text{TiO}_2$ , as it is possible using the sol-gel, therefore excitation under visible light is only possible in the  $\text{WO}_3$  semiconductor. However, under UV-Vis irradiation both, the  $\text{WO}_3$  and  $\text{TiO}_2$  semiconductors can be excited and then the transfer of the electrons from the conductive band of  $\text{TiO}_2$  to  $\text{WO}_3$  is possible, making the separation of free carriers more efficient, which increases the yield of photochemical reactions.

The photoactivity of the prepared  $\text{WO}_3/\text{TiO}_2$  photocatalysts under both, UV and artificial solar light irradiations towards HA decomposition is discussed. The theoretical amount of  $\text{WO}_3$  in  $\text{TiO}_2$  was 3%. This was an optimal value selected on the basis of the previous experiments, also being in a good agreement with the literature data<sup>17,19</sup>.

## EXPERIMENTAL

### Materials

$\text{TiO}_2$  was supplied by the Chemical Factory Police S.A. in Poland. It consists of the anatase phase, around 11.5 wt % and a small amount of rutile phase, about 3.5 wt %, and has high BET surface area, around  $275 \text{ m}^2/\text{g}$ .  $\text{WO}_2$  purchased from Sigma-Aldrich Co. (a.g.) was used as a tungsten precursor. 30%  $\text{H}_2\text{O}_2$  purchased from Scharlau Chemie was used as a dissolving agent in the preparation of  $\text{WO}_3/\text{TiO}_2$ . Leonardite humic acid was purchased from the IHSS (International Humic Substances Society). According to the elemental analyses obtained from the list of IHSS products Leonardite HA standard (IS104H) contains in % (w/w): 63.81 C, 3.70 H, 31.27 O, 1.23 N, 0.76 S, < 0.01 P, and 2.58 ash.

### Photocatalysts preparation

The  $\text{WO}_3/\text{TiO}_2$  photocatalyst was prepared by the impregnation method. After impregnation the samples were calcinated at 400 and 600°C. The theoretical amount of the formed  $\text{WO}_3$  in  $\text{WO}_3/\text{TiO}_2$  was 3 wt.%. For the preparation 3 g of  $\text{TiO}_2$  and 0.084 g of  $\text{WO}_2$  were used. The detailed procedure was already described in the previous paper<sup>22</sup>.

### Characterization of photocatalysts

The phase composition of the photocatalysts was measured by the XRD powder diffraction. The measurements were performed in the X'Pert PRO diffractometer of Philips Company, with the  $\text{CuK}\alpha$  lamp (35 kW, 30mA). The obtained XRD patterns were compared with the JCPDS (Join Committee on Powder Diffraction Standards) cards.

The UV-Vis diffuse reflectance spectra were taken in the Jasco V-530 spectrometer. These spectra were recorded in the range of 250 to 800 nm with  $\text{BaSO}_4$  as a reference and transformed to Kubelka-Munk equation for the indirect semiconductor.

The microstructure of the photocatalysts surface was analysed via a high resolution transmission electron microscope (HR-TEM)-FEI TecnaiF30.

The electrokinetic potential of the photocatalysts surface was measured by the connection of electrophoresis and LDV (Laser Doppler Velocimetry) method in Zetasizer Nano ZS.

The BET surface area was determined by the measurements of nitrogen adsorption and desorption isotherms at 77 K using Autosorb 3 (Quantachrome, U.S.A.) equipment. Prior to the adsorption measurements the samples were degassed for 24 h at 105°C under high vacuum.

The formation of OH radicals on the photocatalysts surface under both, UV and artificial solar light irradiations was measured by the fluorescence method. In this method the photocatalyst is placed into the coumarin solution, where under the irradiation of the light formed on the photocatalyst surface the OH radicals easily react with coumarin to produce a highly fluorescent product, 7-hydroxycoumarin, which was analysed in the fluorescence spectrometer Hitachi F-2500 [22, 31].

### Photocatalytic activity test

The photoactivities of the prepared samples were tested for humic acids (HA) decomposition under the artificial visible light and UV irradiations.

The fluorescence lamp was used as a source of artificial visible light. The measured intensity of the incident light during photoreaction was  $42 \text{ W}/\text{m}^2$  in the range of visible light (350–750 nm) and  $0.8 \text{ W}/\text{m}^2$  in the range of UV. In the case of UV irradiation the Philips solar UV lamp was used. This lamp emits the light at the UV range with the intensity of  $165 \text{ W}/\text{m}^2$  and at the visible region about  $165 \text{ W}/\text{m}^2$ . The photoemission spectra of both lamps are shown in Fig. 1.

The model solution of HA was prepared by dissolving of Leonardite HA in an ultra pure distilled water with addition of a little amount of 1 M NaOH to increase their solubility and followed filtration through the membrane filter of  $0.45 \mu\text{m}$ . The concentration of HA of the prepared solution was estimated on the basis of

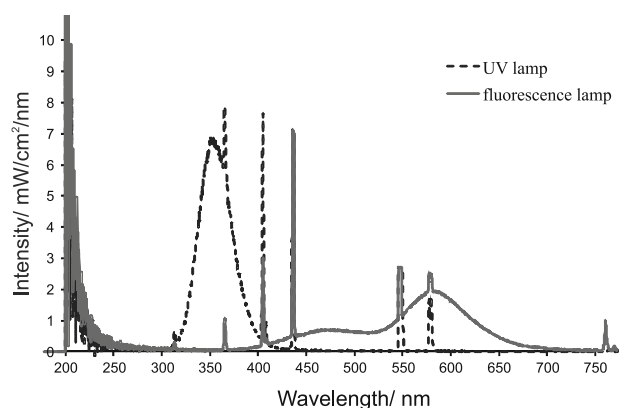


**Figure 1.** The photoemission spectra of UV and fluorescence lamps

TOC analyses and the calculation regarding the content of carbon in HA given by the producer.

HA degradation was performed in a batch type reactor with the suspension of 0.2 g/L photocatalysts and 0.5 L of HA solution with the concentration of around 7 mg/L and 13 mg/L for the artificial solar light and UV irradiations, respectively.

Before irradiation the preliminary adsorption of HA on the samples surface was determined. From the literature it is known that the adsorption equilibrium of HA on the TiO<sub>2</sub> surface is reached within 30 min<sup>5,7,8</sup>. From our previous experiments it was estimated that this equilibrium is reached after around 3 hours<sup>4</sup>.

The solutions were first magnetically stirred in the dark for 3 hours and then were irradiated by 10 and 20 hours under UV and artificial solar light irradiation, respectively.

The changing of TOC in the reaction solution within the irradiation time was measured in the TOC analyser Multi N/C 3100 (Analytik Jena). The TOC analyses were performed for the monitoring of the mineralisation degree of HA after photocatalysis.

The plot of relative TOC changes in the HA solution against irradiation time was approximated to be linear, therefore the rate constant ( $k_{HA}$ ), i.e., the slope of the linear relation, was determined on each sample and used as a measure of its photocatalytic activity.  $K_{HA}$  was determined as zero order kinetic reaction from equation:  $C_{eq}-C = k_{HA} t$

where:

$k_{HA}$  – rate constant of HA mineralisation

$C_{eq}$  – concentration of HA (after adsorption on the photocatalyst surface)

$C$  – concentration of HA after irradiation

## RESULTS

### XRD measurements

In Fig. 2 XRD patterns of TiO<sub>2</sub> original, calcined and modified with WO<sub>3</sub> are presented.

The original TiO<sub>2</sub> showed a poorly crystallized anatase phase with an insignificant amount of rutile. After calcination, the growing of anatase crystals could be observed. That resulted in the narrowing of the peaks, which refers to the anatase phase. Higher calcination temperature gives more sharp anatase reflexes. After the modification of TiO<sub>2</sub> with WO<sub>3</sub> there were not ob-

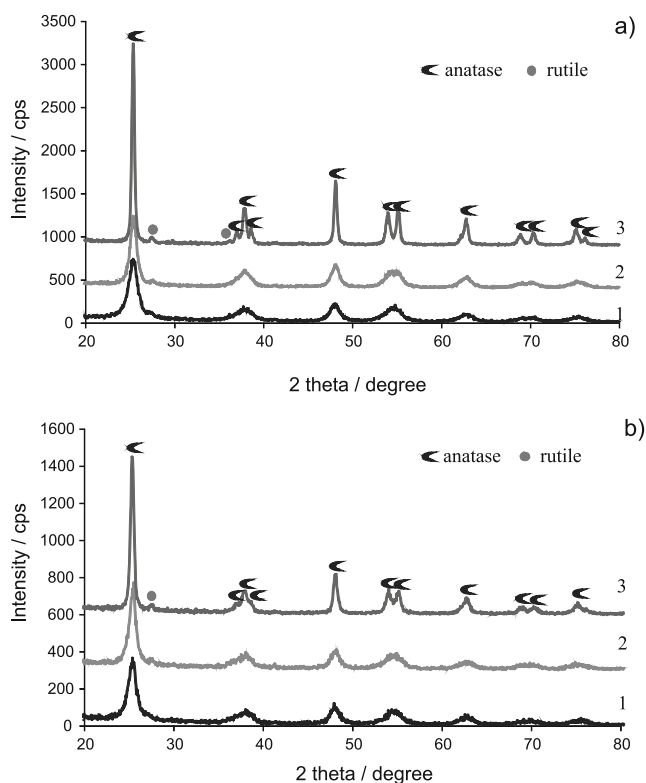


**Figure 2.** The XRD patterns of a) TiO<sub>2</sub> and b) WO<sub>3</sub>/TiO<sub>2</sub> photocatalysts: (1) uncalcined, (2) calcined at 400°C and (3) calcined at 600°C

served any essential changes in the XRD patterns, the tungsten oxides phases were not detected. It could be caused by a good dispersion of tungsten oxides in a bulk of TiO<sub>2</sub> and also a small content of WO<sub>3</sub> in TiO<sub>2</sub> (3 wt %) being out of XRD detection limit. Similar results were reported by Shifu et al.<sup>19</sup>. They concluded that the reflections corresponding to WO<sub>3</sub> were not detected because of its too low concentration, or the presence in the amorphous state or by their strong dispersion in a bulk phase.

In order to check that crystallization of WO<sub>3</sub> occurs at the preparation conditions, tungsten precursor – WO<sub>2</sub>, was dissolved in 30% H<sub>2</sub>O<sub>2</sub> and was treated in a vacuum evaporator without an addition of TiO<sub>2</sub> and then followed calcinations at both, 400 and 600°C. The XRD patterns of the formed WO<sub>3</sub> are shown in Fig. 3.

From the XRD patterns it can be observed that WO<sub>2</sub> in the H<sub>2</sub>O<sub>2</sub> solution underwent insignificant transformation to WO<sub>3</sub> (anorthic phase), which appeared quantitatively

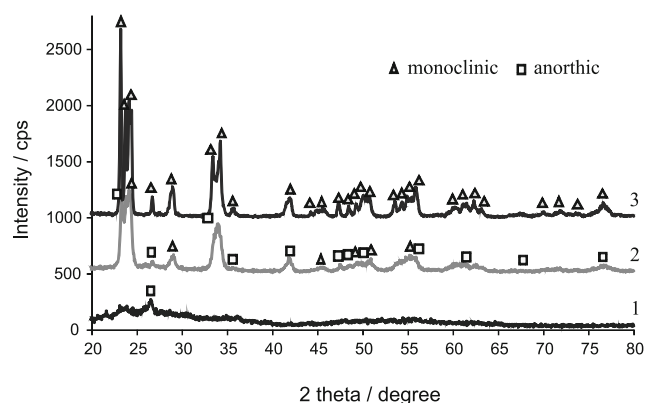


**Figure 3.** The XRD patterns of WO<sub>2</sub> dissolved in H<sub>2</sub>O<sub>2</sub> and treated in vacuum evaporator, 1) uncalcined, 2) calcined at 400°C and 3) calcined at 600°C

after heat treatment at 400°C. At this temperature an insignificant amount of monoclinic phase of  $\text{WO}_3$  was formed as well. At 600°C the only monoclinic  $\text{WO}_3$  phase was observed. Observation of the crystal structure of the prepared  $\text{WO}_3/\text{TiO}_2$  samples was performed by TEM analyses. In Fig. 4 TEM images of original  $\text{TiO}_2$  and  $\text{WO}_3/\text{TiO}_2$  calcined at 600°C are presented.

From the TEM images it is observed that  $\text{TiO}_2$  consists of small particles, with the size below 10 nm, calcination at 600°C caused sintering and the growing of particles, but small anatase crystals of 5 nm size still remain in this  $\text{WO}_3/\text{TiO}_2$  sample. The anatase crystals in  $\text{WO}_3/\text{TiO}_2$  sample are surrounded with an amorphous state, which is most probably connected with doping of tungsten oxides to  $\text{TiO}_2$  but also with the existence of some part of amorphous  $\text{TiO}_2$  particles which did not transform to any crystal phase during the heat treatment.

#### UV-Vis /DR

In Fig. 5 the UV-Vis/DR spectra were shown for  $\text{TiO}_2$ ,  $\text{WO}_3/\text{TiO}_2$  samples before and after calcination at 600°C and for comparison prepared at the same way  $\text{WO}_3$  at 600°C

Modification of  $\text{TiO}_2$  with  $\text{WO}_2$  and  $\text{H}_2\text{O}_2$  caused increase absorption of the visible light in the whole range but the most noticed in the range of 400–550 nm, similar as  $\text{WO}_3$ . Heat treatment of  $\text{WO}_3/\text{TiO}_2$  caused almost a complete reduction of absorption in the visible range. When we compare the spectra of  $\text{TiO}_2$  and  $\text{WO}_3$ , the latter one has shifted the absorption edge to the visible light and as a result its absorption maximum is at 457 nm whereas for  $\text{TiO}_2$  is at 372 nm. It means that this  $\text{WO}_3$  semiconductor can be excited with the visible light, contrary to  $\text{TiO}_2$  and prepared  $\text{WO}_3/\text{TiO}_2$  samples. In our previous studies when we used a higher amount of

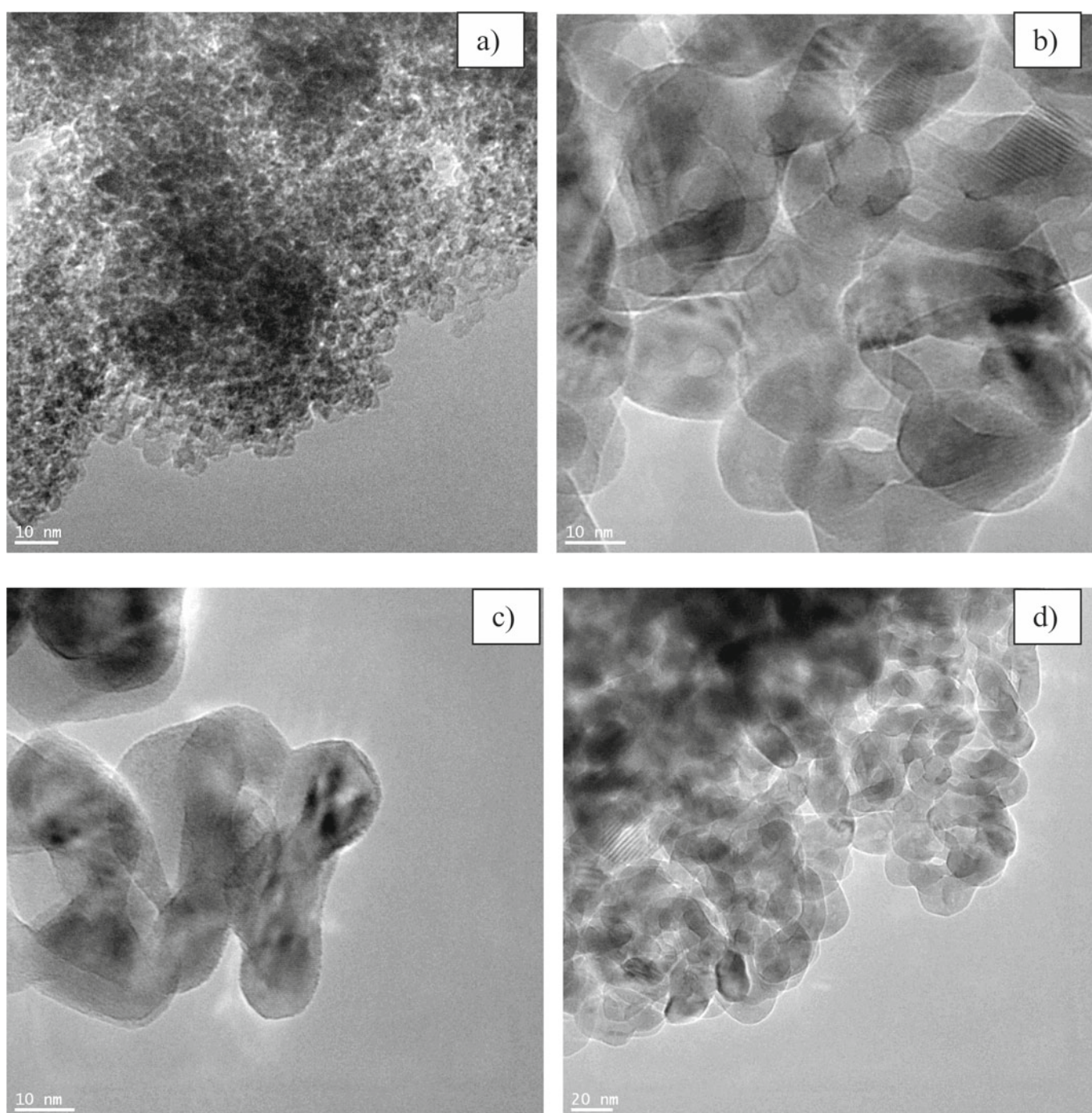


**Figure 4.** TEM images of a)  $\text{TiO}_2$ , and b-d)  $\text{WO}_3/\text{TiO}_2$  calcined at 600°C

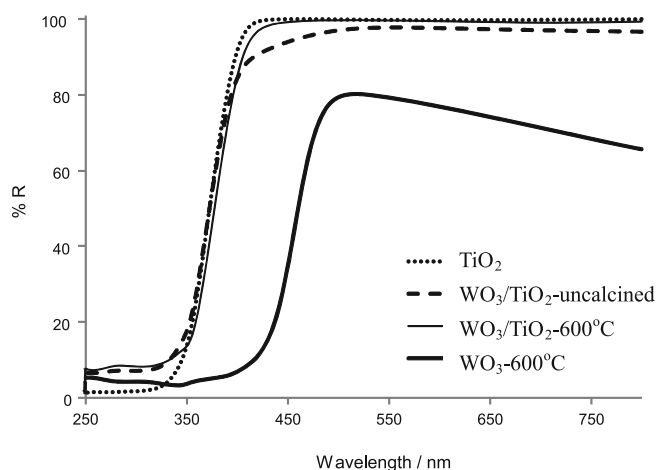


**Figure 5.** UV-Vis/DR spectra of  $\text{TiO}_2$ ,  $\text{WO}_3/\text{TiO}_2$  and  $\text{WO}_3$  samples

$\text{WO}_3$  doped to  $\text{TiO}_2$  samples, they exhibited higher absorption of the visible light even after heat treatment, however their maximum of absorption was close to  $\text{TiO}_2$  sample<sup>22</sup>.

### OH radicals measurements

Detection of OH radicals formed on the photocatalysts surface after excitation with both, UV and artificial solar light irradiations was performed with the use of fluorescence method, i.e. the measurements of 7-hydroxycoumarin, the product of reaction coumarin with OH radicals. In Fig. 6 and 7 the plots showing the formation of 7-hydroxycoumarin within the time of irradiation are shown.

Modification of  $\text{TiO}_2$  by tungsten precursor and  $\text{H}_2\text{O}_2$  caused an increase of the OH radicals formation on the photocatalysts surface in comparison with the original  $\text{TiO}_2$  under both, the artificial solar light and UV irradiation.

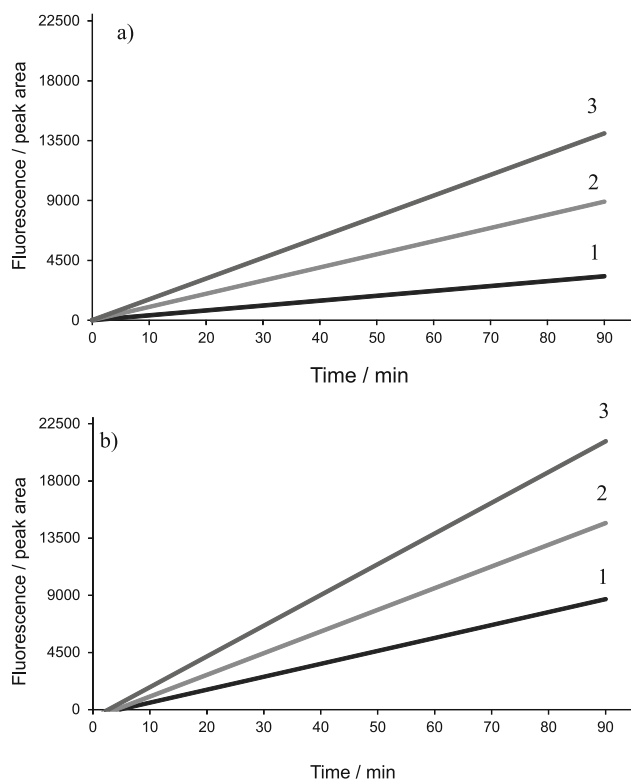


**Figure 6.** The OH radicals formation on: a)  $\text{TiO}_2$  and b)  $\text{WO}_3/\text{TiO}_2$  photocatalysts surface under UV light irradiation: (1) uncalcined, (2) calcined at 400°C and (3) calcined at 600°C

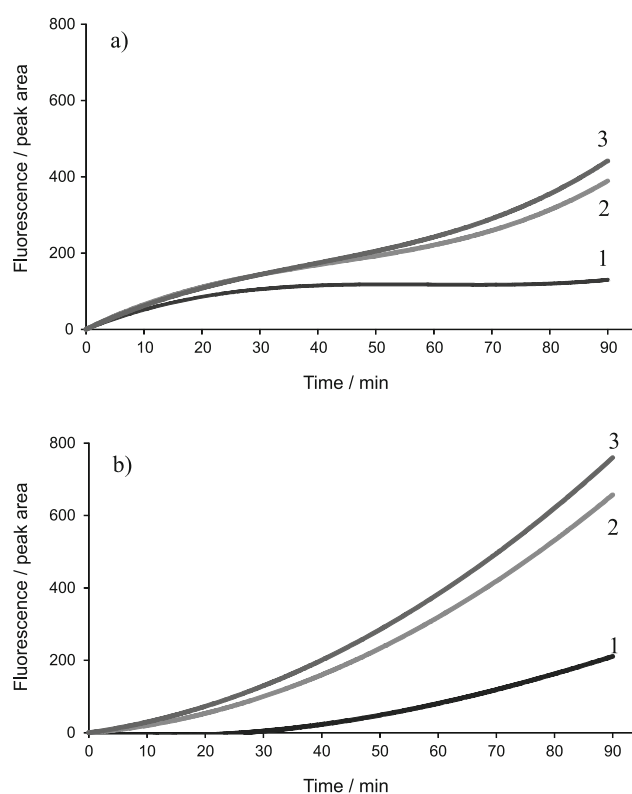


**Figure 7.** The OH radicals formation on: a)  $\text{TiO}_2$  and b)  $\text{WO}_3/\text{TiO}_2$  photocatalysts surface under the artificial solar light irradiation: (1) uncalcined, (2) calcined at 400°C and (3) calcined at 600°C

tions, which could be caused by a better separation of free carriers in the modified samples. The activity of the photocatalysts towards the OH radicals formation under the artificial solar light was incomparably less effective than under UV, it is assumed that this activity was connected just with the excitation of the photocatalysts by a small content of UV light emitted by the fluorescence lamp. With the increase of the heat treatment temperature to 600°C, higher activity towards the OH radicals formation was observed, which can be explained by the growing of anatase crystals, as it was already reported in our previous paper<sup>22</sup>. The linear correlation between the time of UV irradiation and the fluorescence peak of 7-hydroxycoumarin indicates that the amount of OH radicals is proportionally increasing to the irradiation time, under the solar light irradiation the concentration of OH radicals seems to be insignificant and therefore at the beginning the reaction with coumarin does not occur, with the time of irradiation the amount of OH radicals increases and then the product of reaction, 7-hydroxycoumarin appears, at the higher concentration of the OH radicals the trend of this line tends to be linear. Probably for the detection of a small amount of OH radicals the concentration of coumarin was too high. We suppose that for the coupled  $\text{TiO}_2$ - $\text{WO}_3$  photocatalysts injecting of electrons from the conductive band of  $\text{TiO}_2$  to  $\text{WO}_3$  took place, making the  $\text{TiO}_2$  particles more positively charged and improving the separation of free carriers, therefore with the time of irradiation the amount of the formed OH radicals increased rapidly. In Table 1 the values of  $k_{\text{OH}}$  coefficient for the OH radicals formation under the UV irradiation were listed.

**Table 1.** Chemical composition of the spent vanadium catalyst

Properties	Photocatalyst					
	TiO <sub>2</sub>			WO <sub>3</sub> /TiO <sub>2</sub>		
	uncalcined	400°C	600°C	uncalcined	400°C	600°C
Zeta potential [mV]	12	8,6	9,8	-10,3	-15,4	-23,9
S <sub>BET</sub> [m <sup>2</sup> /g]	275	172	51	212,6	185,7	66,3
k <sub>OH</sub> (UV) [min <sup>-1</sup> ] (R <sup>2</sup> )	31,62 (0,97)	94,65 (0,99)	154,15 (0,99)	101,72 (0,98)	170,79 (0,99)	241,91 (0,99)
k <sub>HA</sub> (UV) [mg/dm <sup>3</sup> h] (R <sup>2</sup> )	0,83 (0,99)	0,63 (0,99)	1,51 (0,99)	1,58 (0,99)	0,89 (0,99)	1,12 (0,99)

### Zeta Potential

The values of electrokinetic zeta potentials of the photocatalysts particles measured in the ultra pure water are listed in Table 1.

Modification of TiO<sub>2</sub> by tungsten oxides caused the change of the zeta potential of particles from +12 to -10.3 mV. With an increase of the temperature of the heat treatment the changes were higher in direct minus values. It means that these TiO<sub>2</sub> photocatalysts after a modification with tungsten oxides exhibited the Bronstead acid behaviour. A similar effect was observed by the other authors<sup>26</sup>.

### Measurements of BET surface area

The values of the SBET surface area for the studied photocatalysts are listed in Table 1.

Modification of TiO<sub>2</sub> by tungsten oxides caused that

the SBET surface area decreased from 275 to 212.6 m<sup>2</sup>/g. Calcination of the samples caused the reduction of the BET surface area due to the growth and sintering of the particles. However, the BET surface area of TiO<sub>2</sub> heated at 600°C of around 50 m<sup>2</sup>/g was comparable with the commercially available TiO<sub>2</sub> P25 of Evonik company.

### Photocatalytic decomposition of HA

HA were initially adsorbed on the photocatalyst surface for 3 h (in a dark) and then were irradiated with UV either artificial solar light irradiations. In Fig. 8 and 9 the changes of the TOC concentration after adsorption and during the UV and artificial solar light irradiations for TiO<sub>2</sub> and the WO<sub>3</sub>/TiO<sub>2</sub> samples are presented.

The original TiO<sub>2</sub> showed high adsorption of HA on its surface, around 47.15 mg HA/g of photocatalyst. A

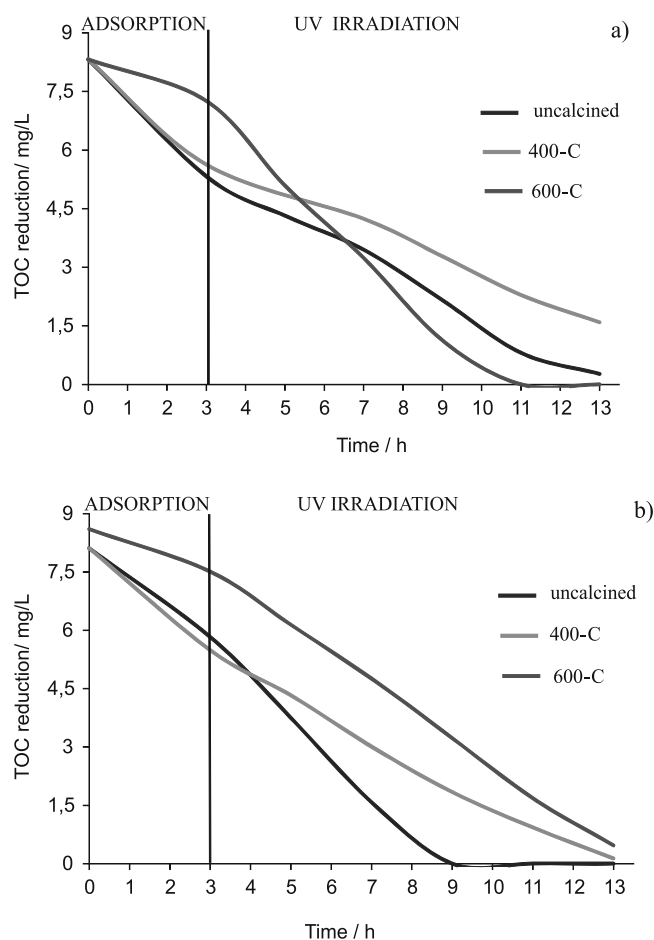


**Figure 8.** Adsorption and photodecomposition of HA under UV irradiation on a) TiO<sub>2</sub> and b) WO<sub>3</sub>/TiO<sub>2</sub> photocatalysts

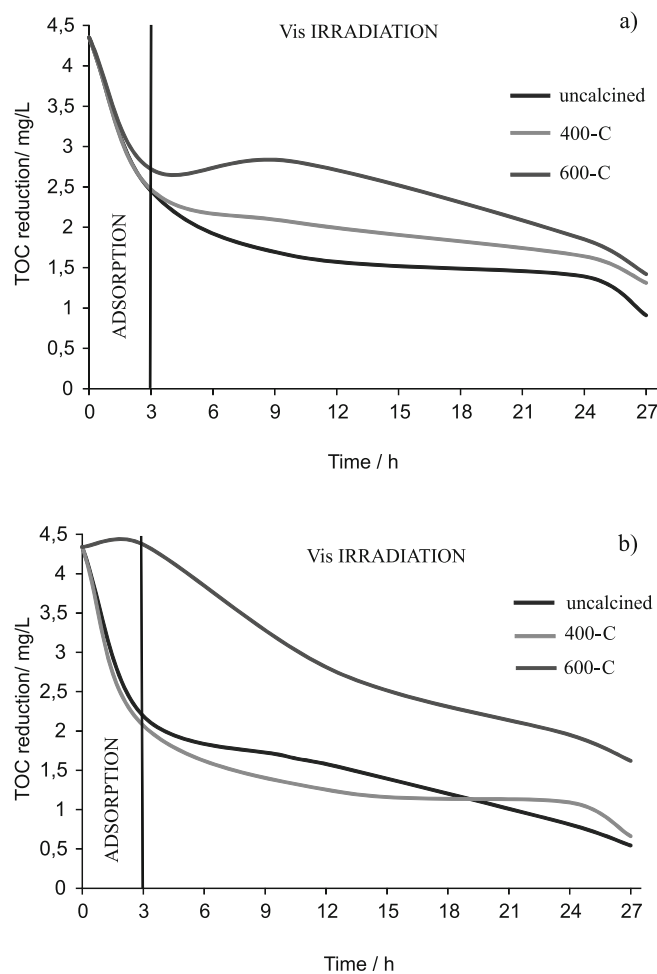


**Figure 9.** Adsorption and photodecomposition of HA under artificial solar light irradiation on a) TiO<sub>2</sub> and b) WO<sub>3</sub>/TiO<sub>2</sub> photocatalysts

similar value of HA adsorption on TiO<sub>2</sub> was obtained by Dziejczak et al.<sup>8</sup>, whereas the other researchers reported the lower values, from 0.7 to 23 mg/g photocatalyst<sup>5,7</sup>. It was reported that adsorption of HA is favored in acid conditions and decreases with the increasing of the pH of the solution<sup>6-8</sup>. In our experiment we used the natural pH of HA solution, which was around 6.6. Doping WO<sub>3</sub> to TiO<sub>2</sub> caused that the adsorption of HA was insignificant lower, around 35.9 mg HA/g of photocatalyst. Calcination of the samples led to a decrease of HA adsorption, what was related to their lower BET surface area in comparison with the uncalcined ones. In general adsorption of HA on the surface of both, TiO<sub>2</sub> and WO<sub>3</sub>/TiO<sub>2</sub> photocatalysts was strongly related to their BET surface area, changing of the electrokinetic potential in the WO<sub>3</sub>/TiO<sub>2</sub> samples did not influence the HA affinity to their surface. The photocatalytic decomposition of HA was performed after its adsorption on the photocatalyst surface, therefore to evaluate the photocatalytic activity of the samples, the concentration of HA after adsorption was taken as an initial concentration of HA. The rate of HA decomposition under UV irradiation was calculated and the values of k<sub>HA</sub> were listed in Table 1. Under artificial solar light irradiation it was difficult to fit the kinetic curve, because the mineralisation degree was not increasing proportionally with the irradiation time. It could be caused by the slowly increasing of the OH radicals during the excitation of the photocatalysts with the visible light. It was reported that the process of HA decomposition does not follow the Langmuir – Hisnshelwood kinetics and is controlled rather by the rate of the generation of the reactive radicals in the photoexcitation process<sup>8</sup>. In our results in the case of TiO<sub>2</sub> there is almost the same relation, the higher amount of the OH radicals formation on TiO<sub>2</sub> calcined at 600°C resulted in a higher mineralisation degree of HA in comparison to uncalcined one TiO<sub>2</sub>. In the case of the WO<sub>3</sub>/TiO<sub>2</sub> samples there is not the same relation, the uncalcined WO<sub>3</sub>/TiO<sub>2</sub> showed the highest mineralisation degree, however this WO<sub>3</sub>/TiO<sub>2</sub> calcined at 600°C (with the highest amount of OH radicals formation) was more active than that calcined at 400°C. Therefore it can be concluded that in the case of the WO<sub>3</sub>/TiO<sub>2</sub> sample the surface oxidative reactions are very important. Cho and Choi<sup>6</sup> reported that since HA is a macromolecule with many redox centers, a series of electron transfers may take place on TiO<sub>2</sub> surface. Although the photoinduced electron-donating (oxidation) property of HA has been mainly discussed so far, the electron-accepting (reduction) property of HA should be also recognized in order to understand the overall process. Sequential electron transfers from excited HA to TiO<sub>2</sub> conductive band could lead to mineralization with CO<sub>2</sub> evolution while the electron transfers from conductive band to HA tend to inhibit the mineralization process<sup>6</sup>. In the case of WO<sub>3</sub>/TiO<sub>2</sub> sample there is a possibility of electron transfer from excited HA to both TiO<sub>2</sub> and WO<sub>3</sub>, and it seems that the transfer to WO<sub>3</sub> plays an important role in HA mineralisation.

To summarize the photocatalytic activity of TiO<sub>2</sub> and WO<sub>3</sub>/TiO<sub>2</sub> photocatalysts, it has to be pointed out that in the case of TiO<sub>2</sub> enhanced photocatalytic activity was observed for the sample calcined at 600°C which revealed

high OH radicals formation. However, in the case of WO<sub>3</sub>/TiO<sub>2</sub> photocatalysts the highest photocatalytic activity was achieved on the uncalcined sample, which showed high adsorption of HA, that could be caused by a better separation of free carriers in TiO<sub>2</sub> and enhanced the yield of surface oxidative reactions. Self-excitation of HA preliminary adsorbed on the surface of the photocatalyst could occur resulting in their fast decomposition, especially under UV irradiation. The photocatalytic activity of the TiO<sub>2</sub> and WO<sub>3</sub>/TiO<sub>2</sub> photocatalysts under artificial solar light was rather poor, and can be assigned to the small content of UV in the incident light and also in the case of WO<sub>3</sub>/TiO<sub>2</sub> photocatalysts, the presence of WO<sub>3</sub>, which can be excited with the visible light. In that case WO<sub>3</sub>/TiO<sub>2</sub> sample calcined at 600°C was the most active due to the highest amount of OH radicals formation in comparison with the other samples.

## CONCLUSIONS

Modification of TiO<sub>2</sub> by WO<sub>3</sub> caused better separation of free carriers which resulted in both, the increased OH radicals formation on the photocatalyst surface and enhanced direct oxidation of HA. Calcination of TiO<sub>2</sub> and WO<sub>3</sub>/TiO<sub>2</sub> photocatalysts at 400 and 600°C caused the increased OH radicals formation but also the reduction of BET surface area. Mineralisation of HA on TiO<sub>2</sub> was dependent on OH radicals formation, being the highest for TiO<sub>2</sub> calcined at 600°C, which revealed the highest OH radicals formation. However, in the case of the WO<sub>3</sub>/TiO<sub>2</sub> photocatalysts high adsorption of HA on the photocatalyst surface facilitated their decomposition under UV irradiation, and the highest decomposition rate of HA was noted for the uncalcined sample. In that case a good separation of free carriers and direct oxidation of HA occurred, which surely accelerated their decomposition. Possible self-excitation of HA under UV irradiation could enhance their decomposition. The prepared WO<sub>3</sub>/TiO<sub>2</sub> photocatalysts did not show narrowing of the band gap and the red shift in the UV/Vis absorption spectra, therefore they were not active under the visible light. The decomposition of HA under the artificial solar light irradiation on WO<sub>3</sub>/TiO<sub>2</sub> photocatalyst calcined at 600°C can be assigned to the small content of UV in the incident light and higher OH radicals formation in comparison with the other samples.

## ACKNOWLEDGEMENTS

This work was supported by the research project from the Ministry of Science and Higher Education Nr. NN 209 200 538.

## LITERATURE CITED

- Murray, C.A. & Parsons, S. (2004). Removal of NOM from drinking water: Fenton's and photo-Fenton's processes. *Chemosphere*. 54, 1017–1023. DOI: 10.1016/j.chemosphere.2003.08.040.
- Libeck, B. (2011). The effectiveness of humic acids coagulation with the use of cationic polyacrylamides. *Water Science & Technology* 63, 1944–1949. DOI: 10.2166/wst.2011.194
- Wei, M.C., Wang, K.S., Hsiao, T.E., Lin, I.C., Wu, H.J., Wu, Y.L., Liu, P.H. & Chang, S.H. (2011). Effects of UV irradiation on humic acid removal by ozonation, Fenton

- and Fe<sup>0</sup>/air treatment: THMFP and biotoxicity evaluation. *Journal of Hazardous Materials* 195, 324–31. DOI: 10.1016/j.jhazmat.2011.08.044
4. Tryba, B., Brożek, P., Piszcz, M. & Morawski, A.W. (2011). New photocatalyst for decomposition of humic acids in photocatalysis and photo-Fenton processes. *Polish Journal of Chemical Technology* 13, 8–4. DOI: 10.2478/v10026-011-0042-5.
5. Wiszniowski, J., Didier, R., Surmacz-Gorska, J. & Miksch, K. (2002). Photocatalytic decomposition of humic acids on TiO<sub>2</sub>: Part I: Discussion of adsorption and mechanism. *J. Photochem. Photobiol. A: Chem.* 152, 267–273.
6. Cho, Y. & Choi, W. (2002). Visible-light induced reactions of humic acids on TiO<sub>2</sub>. *J. Photochem. Photobiol. A: Chem.* 148, 129–135.
7. Xuea, G., Liua, H., Chena, Q., Hills, C., Tyrerc, M. & Innocenta, F. (2011). Synergy between surface adsorption and photocatalysis during degradation of humic acid on TiO<sub>2</sub>/activated carbon composites. *Journal of Hazardous Materials* 186, 765–772. DOI: 10.1016/j.jhazmat.2010.11.063.
8. Dzedzic, J., Wodka, D., Nowak, P., Warszyński, P., Simon, C. & Kumakiri, I. (2010). Photocatalytic Degradation of the humic species as a method of their removal from water – comparison of UV and artificial sunlight irradiation. *Physicochem. Probl. Miner. Process.* 45, 15–28.
9. Seery, M.K., George, R., Floris, P., Pillai, S.C. (2007). Silver doped titanium dioxide nanomaterials for enhanced visible light photocatalysis. *J. Photochem. Photobiol. A: Chem.* 189, 258. DOI:10.1016/j.jphotochem.2007.02.010.
10. Selvam, P., Kumar, S., Sivakumar, R., Anandan, S., Madhavan, J., Maruthamuthu, P., Ashokkumar, M. (2008). Photocatalytic degradation of Acid Red 88 using Au–TiO<sub>2</sub> nanoparticles in aqueous solutions. *Water Res.* 42 4878–4884. DOI:10.1016/j.watres.2008.09.027.
11. Kim S., Lee, S. (2009). Visible light-induced photocatalytic oxidation of 4-chlorophenol and dichloroacetate in nitrated Pt-TiO<sub>2</sub> aqueous suspensions, *J. Photochem. Photobiol. A: Chem.* 203, 145–150. DOI:10.1016/j.jphotochem.2009.01.011
12. Shen, H., Mi, L., Xu, P., Shen, W. & Pei-Nan, W. (2007). Visible-light photocatalysis of nitrogen-doped TiO<sub>2</sub> nanoparticulate films prepared by low-energy ion implantation. *Appl. Surf. Sci.*, 253, 7024–7028. DOI:10.1016/j.apsusc.2007.02.023.
13. Janus, M., Choina, J. & Morawski, A.W. (2009). Azo dyes decomposition on new nitrogen-modified anatase TiO<sub>2</sub> with high adsorptivity. *J. Hazard. Mater.* 166, 1–5. DOI:10.1016/j.jhazmat.2008.11.024.
14. Shen, M., Wu, Z., Huang, H., Du, Y., Zou, Z. & Yang, P. (2006). Carbon-doped anatase TiO<sub>2</sub> obtained from TiC for photocatalysis under visible light irradiation. *Mat. Lett.* 60, 693–697. DOI:10.1016/j.matlet.2005.09.068.
15. Janus, M., Tryba, B., Kusiak, E., Tsumura, T., Toyoda, M., Inagaki, M., Morawski, A.W. (2009). TiO<sub>2</sub> nanoparticles with high photocatalytic activity under visible light. *Catal. Lett.* 128, 36–39. DOI: 10.1007/s10562-008-9721-0.
16. Wang, P., Yap, P.S. & Lim, T.T. (2011). C–N–S tridoped TiO<sub>2</sub> for photocatalytic degradation of tetracycline under visible-light irradiation. *Appl. Catal. A* 399, 252–261.
17. Li, X.Z., Li, F.B., Yang, C.L. & Ge, W.K. (2001). Photocatalytic activity of WO<sub>x</sub>-TiO<sub>2</sub> under visible light irradiation. *J. Photochem. Photobiol. A: Chem.* 141, 209–217. DOI:10.1016/S1010-6030(01)00446-4.
18. Song, H., Jiang, H., Liu, X. & Meng, G. (2006). Efficient degradation of organic pollutant with WO<sub>x</sub> modified nano TiO<sub>2</sub> under visible irradiation. *J. Photochem. Photobiol. A: Chem.* 181, 421. DOI:10.1016/j.jphotochem.2006.01.001.
19. Shifu, C., Lei, C., Shen, G. & Gengyu, C. (2005). The preparation of coupled WO<sub>3</sub>/TiO<sub>2</sub> photocatalyst by ball milling. *Powd. Technol.* 160, 198–202. DOI:10.1016/j.powtec.2005.08.012
20. Yang, H., Shi, R., Zhang, K., Hu, Y., Tang, A., Li, X. (2005). Synthesis of WO<sub>3</sub>/TiO<sub>2</sub> nanocomposites via sol-gel method. *J. Alloy. Comp.* 398, 200. DOI:10.1016/j.jallcom.2005.02.002.
21. Ke, D., Liu, H., Peng, T., Liu, X. & Dai, K. (2008). Preparation and photocatalytic activity of WO<sub>3</sub>/TiO<sub>2</sub> nanocomposite particles. *Matt. Lett.* 62, 447. DOI: 10.1016/j.matlet.2007.05.060.
22. Tryba B., Piszcz M. & Morawski A.W. (2009). Photocatalytic activity of TiO<sub>2</sub>-WO<sub>3</sub> composites. *Int. J. Photoenergy.* Article ID 297319. DOI:10.1155/2009/297319.
23. Hathway, T., Rockefeller, E.M., Oh, Y.C., Jenks, W.S. (2009). Photocatalytic degradation using tungsten-modified TiO<sub>2</sub> and visible light: Kinetic and mechanistic effect using multiple catalyst doping strategies. *J. Photochem. Photobiol. A: Chem.* 207, 197–203. DOI:10.1016/j.jphotochem.2009.07.010.
24. Saepurahman, Abdullah, M.A. & Chong, F.K. (2010). Preparation and characterization of tungsten-loaded titanium dioxide photocatalyst for enhanced dye degradation. *J. Hazard. Mater.* 176, 451–458. DOI:10.1016/j.jhazmat.2009.11.050.
25. Sajjad, A.K.L., Shamaila, S., Tian, B., Chen, F. & Zhang, J. (2010). Comparative studies of operational parameters of degradation of azo dyes in visible light by highly efficient WO<sub>x</sub>/TiO<sub>2</sub> photocatalyst. *J. Hazard. Mater.* 177, 781–791. DOI:10.1016/j.jhazmat.2009.12.102.
26. Akurati, K.K., Vital, A., Delleman, J., Michalow, K., Graule, T., Ferri, D., Baiker, A. (2008). Flame-made WO<sub>3</sub>/TiO<sub>2</sub> nanoparticles: Relation between surface acidity, structure and photocatalytic activity. *Appl. Catal. B* 79, 53. DOI:10.1016/j.apcatb.2007.09.036.
27. Piszcz, M., Tryba, B., Grzmil, B. & Morawski, A.W. (2009). Photocatalytic removal of phenol under UV irradiation on WO<sub>x</sub>-TiO<sub>2</sub> prepared by sol-gel method. *Catal. Lett.* 128, 190–196. DOI: 10.1007/s10562-008-9730-z.
28. Kim, T., Burrows, A., Kiely, C.J., Wachs, I.E. (2007). Molecular/electronic structure-surface acidity relationships of model-supported tungsten oxide catalysts. *J. Catal.* 246, 370–381. DOI:10.1016/j.jcat.2006.12.018.
29. Kwon, Y.T., Song, K.Y., Lee, W.I., Choi, G.J. & Do, Y.R. (2000). Photocatalytic behavior of WO<sub>3</sub>-loaded TiO<sub>2</sub> in an oxidation reaction. *J. Catal.* 191, 192–199. DOI:10.1006/jcat.1999.2776.
30. Yang, H., Zhang, D. & Wang, L. (2002). Synthesis and characterization of tungsten oxide-doped titania nanocrystallites. *Matt. Lett.* 57, 674–678. DOI:10.1016/S0167-577X(02)00852-2.
31. Ishibashi, K., Fujishima, A., Watanabe, T., Hashimoto, K., (2000). Detection of active oxidative species in TiO<sub>2</sub> photocatalysis using the fluorescence technique. *Electrochem. Commun.* 2, 207. DOI:10.1016/S1388-2481(00)00006-0.